Mechanistic Studies of the Reaction of Reduced Methane Monooxygenase Hydroxylase with Dioxygen and Substrates

Ann M. Valentine, Shannon S. Stahl, and Stephen J. Lippard*

Contribution from the Department of Chemistry, Massachusetts Institute of Technology, Cambridge, Massachusetts 02139

Received November 16, 1998

Abstract: Soluble methane monooxygenase (sMMO) catalyzes the oxidation of methane to methanol. Single-turnover reactions of sMMO from *Methylococcus capsulatus* (Bath) were studied by stopped-flow optical spectroscopy to examine further the activated dioxygen intermediates and their reactions with hydrocarbon substrates. A diiron(III) peroxo species designated H_{peroxo} is the first intermediate observed in the reaction between the chemically reduced hydroxylase (H_{red}) and dioxygen. The optical spectrum of this species determined by diode array detection is presented for the first time and exhibits visible absorption bands with $\lambda_{max} \approx 420$ nm ($\epsilon = 4000\ M^{-1}\ cm^{-1}$) and $\lambda_{max} = 725$ nm ($\epsilon = 1800\ M^{-1}\ cm^{-1}$). The temperature dependences of the rate constants for formation and decay of H_{peroxo} and for the subsequent intermediate, Q, were examined in the absence and in the presence of hydrocarbon substrates, and activation parameters for these reactions were determined. For single-turnover reaction kinetics monitored at 420 nm, the λ_{max} for Q, a nonlinear Eyring plot was obtained when acetylene or methane was present in sufficiently high concentration. This behavior reflects a two-step mechanism, Q formation followed by Q decay, in which the rate-determining step changes depending on the temperature. The rate of H_{peroxo} formation does not depend on dioxygen concentration, indicating that an effectively irreversible step involving dioxygen precedes formation of the diiron(III) peroxo species. The rate constant observed at 4 °C for H_{peroxo} formation, $1-2\ s^{-1}$, is slower than that determined previously by Mössbauer and optical spectroscopy, $\sim 20-25\ s^{-1}$ (Liu, K. E.; et al. *J. Am. Chem. Soc.* **1995**, *117*, 4997−4998; 10174−10185). Possible explanations for this discrepancy include the existence of two distinct peroxo species. Intermediate Q exhibits photosensitivity when monitored by diode array methodology, a property that may arise from enhanced reactivity of a transient charge-transfer species. The photoreaction can be avoided by using a monochromator to obtain kinetics data at single wavelengths. The reactions of substrates with intermediate species were studied by single- and double-mixing stopped-flow spectroscopy. The Q decay rate exhibits an approximate first-order dependence on substrate concentration for a wide range of hydrocarbons, the relative reactivity varying according to the sequence acetylene > ethylene > ethane > methane > propylene > propane. In addition, the data indicate that H_{peroxo} can oxidize olefins but not acetylene or saturated hydrocarbons.

Introduction

Soluble methane monooxygenase (sMMO) effects the reductive activation of dioxygen and the oxidation of methane according to eq 1.[1,2] In methanotrophic organisms from which

$$CH_4 + O_2 + NADH + H^+ \rightarrow CH_3OH + H_2O + NAD^+ \quad (1)$$

sMMO is isolated, this reaction represents the first step in the assimilation of carbon and energy for the cell.[3,4] The protein system from *Methylococcus capsulatus* (Bath), which operates at 45 °C, includes a 251-kDa hydroxylase (MMOH),[5−8] which is an $\alpha_2\beta_2\gamma_2$ homodimer containing one dinuclear non-heme iron center in each α subunit. A 38.5-kDa reductase protein (MMOR) supplies reducing equivalents to these centers during catalytic turnover.[5,9] Finally, a 15.8-kDa component lacking cofactors (MMOB) acts as a coupling protein,[10−12] linking electron consumption with hydrocarbon oxidation (eq 1).

An early step in the catalytic cycle is reduction of active-site iron to the diferrous state (H_{red}) by electrons from MMOR. Alternatively, the diiron center can be chemically reduced under anaerobic conditions, facilitating study of the reaction between H_{red} and dioxygen by rapid-mixing techniques. Such single-turnover investigations of MMOH from *M. capsulatus* (Bath)[11,13,14] and *Methylosinus trichosporium* (OB3b)[15,16] have

* To whom correspondence should be addressed.

(1) Liu, K. E.; Lippard, S. J. In *Advances in Inorganic Chemistry*; Sykes, A. G., Ed.; Academic Press: San Diego, CA, 1995; Vol. 42, pp 263−289.
(2) Wallar, B. J.; Lipscomb, J. D. *Chem. Rev.* **1996**, *96*, 2625−2657.
(3) Anthony, C. *The Biochemistry of Methylotrophs*; Academic Press: New York, 1982; pp 296−379.
(4) Dalton, H. *Adv. Appl. Microbiol.* **1980**, *26*, 71−87.
(5) Colby, J.; Dalton, H. *Biochem. J.* **1978**, *171*, 461−468.
(6) Woodland, M. P.; Dalton, H. *J. Biol. Chem.* **1984**, *259*, 53−59.
(7) Rosenzweig, A. C.; Frederick, C. A.; Lippard, S. J.; Nordlund, P. *Nature* **1993**, *366*, 537−543.
(8) Rosenzweig, A. C.; Nordlund, P.; Takahara, P. M.; Frederick, C. A.; Lippard, S. J. *Chem. Biol.* **1995**, *2*, 409−418.
(9) Colby, J.; Dalton, H. *Biochem. J.* **1979**, *177*, 903−908.
(10) Green, J.; Dalton, H. *J. Biol. Chem.* **1985**, *260*, 15795−15801.
(11) Liu, K. E.; Valentine, A. M.; Wang, D.; Huynh, B. H.; Edmondson, D. E.; Salifoglou, A.; Lippard, S. J. *J. Am. Chem. Soc.* **1995**, *117*, 10174−10185.
(12) Gassner, G. T.; Lippard, S. J. Unpublished results.
(13) Liu, K. E.; Wang, D.; Huynh, B. H.; Edmondson, D. E.; Salifoglou, A.; Lippard, S. J. *J. Am. Chem. Soc.* **1994**, *116*, 7465−7466.
(14) Liu, K. E.; Valentine, A. M.; Qiu, D.; Edmondson, D. E.; Appelman, E. H.; Spiro, T. G.; Lippard, S. J. *J. Am. Chem. Soc.* **1995**, *117*, 4997−4998; **1997**, *119*, 11134 (Correction).

10.1021/ja9839522 CCC: $18.00
Published on Web 04/09/1999

Scheme 1

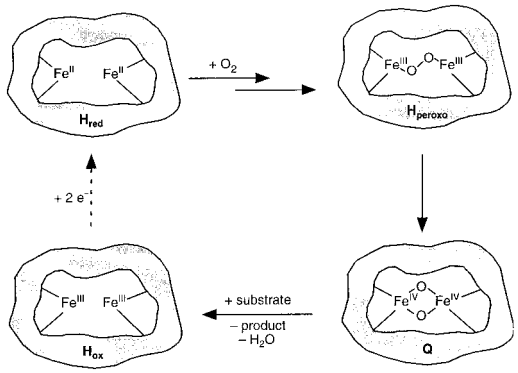

revealed the formation of several intermediates during the reaction cycle. These species have been detected by continuous and discontinuous techniques and both in the presence and in the absence of substrates.

Scheme 1 portrays intermediates observed spectroscopically in the reaction of H_{red} in the presence of 2 equiv of MMOB (H_{red}/2B) with dioxygen. In the absence of MMOB, the oxidation of the diiron center is too slow to be catalytically competent, and intermediate species are not observed. When MMOB is present, the first intermediate appears with a rate constant of ~25 s^{-1} at 4 °C when monitored by rapid freeze quench (RFQ) Mössbauer or optical spectroscopy.[11,13,14] Its properties, when compared to those of well-characterized model compounds,[17−19] are characteristic of a diiron(III) peroxo intermediate, termed H_{peroxo}.

The H_{peroxo} intermediate subsequently converts to a formally high-valent, diiron(IV) intermediate, Q, characterized by its intense yellow color, $\lambda_{max} = 420$ nm, and relatively long lifetime, $k_{form} = 0.45\ s^{-1}$ and $k_{decay} = 0.05\ s^{-1}$ at 4 °C for *M. capsulatus* (Bath).[11,13,15,16] The Mössbauer parameters of Q are most consistent with Fe(IV) centers which, in the *M. capsulatus* (Bath) hydroxylase, appear to be in slightly inequivalent environments.[11,13] RFQ-extended X-ray absorption fine structure (EXAFS) experiments on Q from *Ms. trichosporium* OB3b support a short (~2.45 Å) Fe···Fe distance.[20] The rate of Q decay is greatly accelerated in the presence of substrates, leading to its assignment as the active oxidizing species.[16] The spectroscopic characteristics of H_{peroxo} and Q suggest a range of possible structures,[21] which have been evaluated by theoretical studies employing extended Hückel and density functional calculations.[22−24]

Although conversion of methane to methanol is the physiologically relevant reaction, sMMO can oxidize a wide variety of substrates, including alkanes, alkenes, alkynes, aromatic compounds, and heterocycles.[4,25−27] Substrates range in size from methane to 1,1-diphenyl-2-methylcyclopropane, one of the radical clock substrate probes.[28] Alkenes are epoxidized by sMMO, and some substrates, such as 2-butene, can be either hydroxylated or epoxidized. The α-olefins, propylene and 1-butene, are exclusively epoxidized, however.[25] Acetylene has been characterized as a suicide substrate for sMMO.[29] An interesting and unanswered question is whether and/or how the mechanisms for these oxidation processes differ.

The work described here was undertaken to define further the spectroscopic features of the observable intermediate species, H_{peroxo} and Q, and to characterize their reactions with a range of substrate molecules. Specifically, we provide new information about the following questions. Is H_{peroxo} the first diiron reaction product when H_{red} is mixed with dioxygen? What is the chemical nature of the intermediates characterized spectroscopically? What drives the formation and decay of these species? How do they react in the presence and absence of exogenous substrate? And finally, is the oxidation mechanism the same for all substrates? Such information is essential for a complete understanding of the sMMO system and pertinent to the more general subjects of dioxygen activation and hydrocarbon functionalization by metalloenzymes and biomimetic systems.

Experimental Section

Protein Isolation and Characterization. Native MMOH was purified by a modification of a published procedure[30] reported in detail elsewhere.[31] The purified enzyme was characterized according to methods previously described.[28,32] Specific activity, as measured for propylene oxidation, was in the range of 250−350 munits/mg. Recombinant MMOB was expressed,[33] purified, and characterized according to published procedures.[28]

Single-Turnover Reactions. Preparation of H_{red}. Solutions of MMOH with 2 equiv of MMOB were made anaerobic and reduced as reported elsewhere.[11] The excess dithionite and electron-transfer mediator were removed by two 1-h anaerobic dialyses against 500 mL of 25 mM MOPS (pH 7) in a Vacuum Atmospheres chamber. The solution was diluted to a final MMOH concentration of 75−100 μM for single-mixing and 160−200 μM for double-mixing stopped-flow optical studies. During the experiment, the protein was diluted by a factor of 2 in the single-mixing experiments and by a factor of 4 in those employing double-mixing.

Stopped-Flow Spectroscopy. Both single- and double-mixing stopped-flow experiments were carried out by using a Hi-Tech Scientific (Salisbury, UK) SF-61 DX2 sample handling unit and a diode array spectrophotometer or photomultiplier assembly manufactured by Hi-Tech. The sample handling unit was made anaerobic by passing at least 10 mL of anaerobic dithionite-saturated buffer (25 mM MOPS, pH 7) through the system, followed by at least 20 mL of anaerobic buffer to rinse away the excess dithionite. Anaerobic buffers and protein solutions were transferred by using Hamilton gastight Samplelock syringes. The

(15) Lee, S.-K.; Fox, B. G.; Froland, W. A.; Lipscomb, J. D.; Münck, E. *J. Am. Chem. Soc.* **1993**, *115*, 6450−6451.
(16) Lee, S.-K.; Nesheim, J. C.; Lipscomb, J. D. *J. Biol. Chem.* **1993**, *268*, 21569−21577.
(17) Kim, K.; Lippard, S. J. *J. Am. Chem. Soc.* **1996**, *118*, 4914−4915.
(18) Ookubu, T.; Sugimoto, H.; Nagayama, T.; Masuda, H.; Sato, T.; Tanaka, K.; Maeda, Y.; Okawa, H.; Hayashi, Y.; Uehara, A.; Suzuki, M. *J. Am. Chem. Soc.* **1996**, *118*, 701−702.
(19) Dong, Y.; Yan, S.; Young, V. G., Jr.; Que, L., Jr. *Angew. Chem., Int. Ed. Engl.* **1996**, *35*, 618−620.
(20) Shu, L.; Nesheim, J. C.; Kauffmann, K.; Münck, E.; Lipscomb, J. D.; Que, L., Jr. *Science* **1997**, *275*, 515−518.
(21) Valentine, A. M.; Lippard, S. J. *J. Chem. Soc., Dalton Trans.* **1997**, 3925−3931.
(22) Siegbahn, P. E. M.; Crabtree, R. H. *J. Am. Chem. Soc.* **1997**, *119*, 3103−3113.
(23) Yoshizawa, K.; Ohta, T.; Yamabe, T.; Hoffmann, R. *J. Am. Chem. Soc.* **1997**, *119*, 12311−12321.
(24) Yoshizawa, K.; Yamabe, T.; Hoffmann, R. *New J. Chem.* **1997**, *21*, 151−161.
(25) Colby, J.; Stirling, D. I.; Dalton, H. *Biochem. J.* **1977**, *165*, 395−402.
(26) Green, J.; Dalton, H. *J. Biol. Chem.* **1989**, *264*, 17698−17703.
(27) Fox, B. G.; Borneman, J. G.; Wackett, L. P.; Lipscomb, J. D. *Biochemistry* **1990**, *29*, 6419−6427.
(28) Liu, K. E.; Johnson, C. C.; Newcomb, M.; Lippard, S. J. *J. Am. Chem. Soc.* **1993**, *115*, 939−947.
(29) Prior, S. D.; Dalton, H. *FEMS Microbiol. Lett.* **1985**, *29*, 105−109.
(30) Fox, B. G.; Froland, W. A.; Jollie, D. R.; Lipscomb, J. D. In *Methods in Enzymology*; Academic Press: New York, 1990; Vol. 188, pp 191−202.
(31) Willems, J.-P.; Valentine, A. M.; Gurbiel, R.; Lippard, S. J.; Hoffman, B. M. *J. Am. Chem. Soc.* **1998**, *120*, 9410−9416.
(32) DeWitt, J. G.; Bentsen, J. G.; Rosenzweig, A. C.; Hedman, B.; Green, J.; Pilkington, S.; Papaefthymiou, G. C.; Dalton, H.; Hodgson, K. O.; Lippard, S. J. *J. Am. Chem. Soc.* **1991**, *113*, 9219−9235.
(33) Coufal, D. E.; Blazyk, J.; Whittington, D. A.; Wu, W. W.; Lippard, S. J. Manuscript in preparation.

temperature was thermostated with a circulating water bath. In experiments with varying temperatures, solutions were allowed to equilibrate for at least 10 min before beginning the run. Matheson gas mixers were used as reported previously[11] to prepare solutions of known dioxygen concentration.

In experiments employing gaseous substrates, buffer solutions were sparged at 25 °C with the appropriate substrate for 30 min or more, and the saturating substrate concentration was calculated.[34] The solutions were diluted to achieve the desired substrate concentration by using gastight syringes fitted with three-way valves.

In single-mixing experiments, reduced anaerobic protein solutions were mixed rapidly with dioxygen-containing solutions with or without substrate. In double-mixing experiments, the reduced protein was mixed with dioxygen-containing buffer in the first push, and then, after a programmed delay time, substrate-containing buffer was introduced in the second push, filling the optical cell and initiating data collection. Data were obtained with the KinetAsyst software package (Hi-Tech) and analyzed with this program as well as Specfit[35] for global analysis. The Specfit package performs a principal component analysis by singular value decomposition to yield orthogonal spectral and time axis eigenvectors. These vectors were examined and applied by global Marquardt least-squares fits to the appropriate kinetic model. The spectra of intermediate species and rate constants were derived from such fits.

Quantitation of Hydrogen Peroxide. The production of hydrogen peroxide during a single turnover was investigated by a modification of a published method.[36] A 50 μM sample of MMOH in 25 mM MOPS (pH 7) was reduced according to the usual procedure (see above) in the presence or in the absence of 100 μM MMOB, and the dithionite and methyl viologen were dialyzed away anaerobically. The solutions were diluted with an equal volume of dioxygen-saturated buffer. After 60 s, 100 μL of a 2 M solution of trichloroacetic acid was added to each 450-μL sample to quench the reaction. A 50-μL portion of 100 mM $Fe(NH_4)_2(SO_4)_2 \cdot 6H_2O$ and 500 μL of 2.5 M NaSCN were added, and the resulting absorbance at 480 nm was compared to those of a series of standard samples to quantitate the amount of hydrogen peroxide produced.

Detection of Products in the Propylene Reaction. The products of propylene oxidation in a single-turnover reaction were determined by using gas chromatography (GC) with flame ionization detection as described elsewhere.[32] Authentic samples of propylene oxide and 3-hydroxy-1-propene were employed to construct calibration curves.

Results

Optical Spectra of Intermediate Species. Figure 1 depicts the optical spectra observed after mixing H_{red}/2B with dioxygen in the absence of substrate at 20 °C. A total of 200 spectra were collected in a typical run. The data were fit well by an A → B → C → D kinetic model (A = H_{red}, B = H_{peroxo}, C = Q, D = H_{ox}) with the Specfit software package,[35] yielding the spectra presented in Figure 2A. The rate constants determined by this global analysis method were $k_1 = 40 \pm 3$ s^{-1}, $k_2 = 9.9 \pm 1.0$ s^{-1}, and $k_3 = 0.31 \pm 0.05$ s^{-1}. Each of these values is compatible with the results of steady-state turnover kinetics, for which a k_{cat} of 0.19 s^{-1} is observed at 45 °C.[37] Based on these rate constants, the time-dependent evolution of intermediates depicted in Figure 2B was obtained. Difference spectra, prepared by subtracting the diode array spectrum of H_{ox} from those for

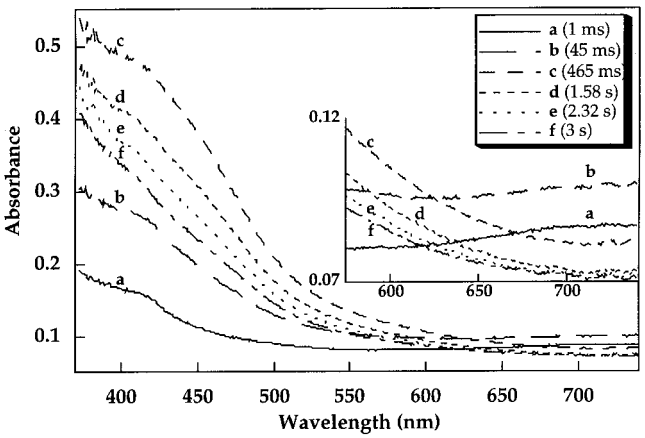

Figure 1. Diode array data collected after the rapid mixing of H_{red}/2B with dioxygen at 20 °C in 25 mM MOPS (pH 7). H_{red} and dioxygen concentrations were 50 and 0.5 mM, respectively, after mixing. Two hundred spectra were collected in a typical experiment. Selected spectra are shown.

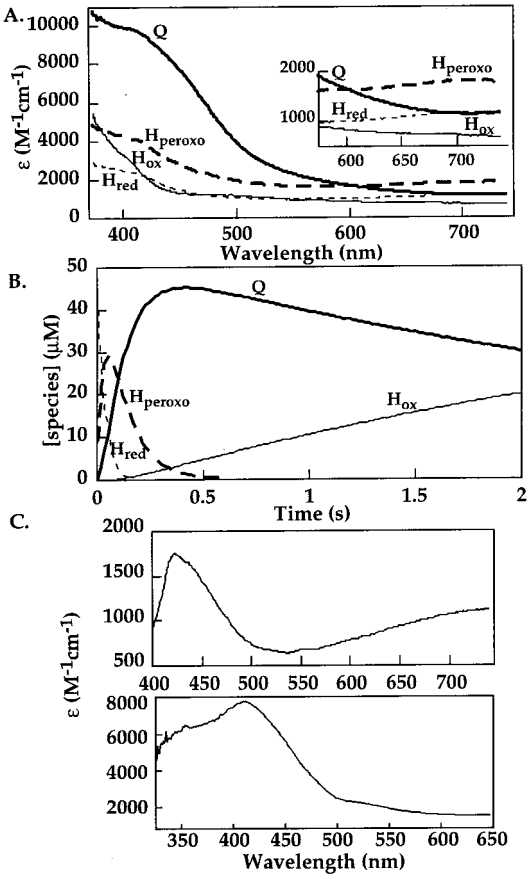

Figure 2. Fits of the data from Figure 2 with the global analysis package Specfit. The optical species (A) evolve with $k_1 = 40$ s^{-1}, $k_2 = 9.9$ s^{-1}, and $k_3 = 0.31$ s^{-1}, where the rate constants describe H_{peroxo} formation, H_{peroxo} decay/Q formation, and Q decay, respectively. (B) Time evolution of species with these rate constants. (C) Spectra prepared by subtracting the H_{ox} spectrum from that of H_{peroxo} (top) and Q (bottom).

H_{peroxo} and Q, revealed the distinct optical features of these transient intermediates (Figure 2C).[38]

Studies of Q Formation and Decay in the Absence of Substrates. The chemical reaction responsible for the decay of Q in the absence of substrate is not well understood. No covalent protein adducts have been detected, indicating that no single amino acid side chain has been oxidized.[39,40] Hydrogen peroxide

(34) Wilhelm, E.; Battino, R.; Wilcock, R. J. *Chem. Rev.* **1977**, *77*, 219−262.

(35) Binstead, R., Specfit Global Analysis Package, 2.10M, Chapel Hill, NC, 1997.

(36) Hildebrandt, A. G.; Roots, I. *Arch. Biochem. Biophys.* **1975**, *171*, 385−397.

(37) Green, J.; Dalton, H. *Biochem. J.* **1986**, *236*, 155−162.

Table 1. Activation Parameters for the Formation and Decay of Intermediate Species

entry	rate constant[a]	$\Delta H^{\ddagger}$ (kcal/mol)	$\Delta S^{\ddagger}$ (cal/mol·K)	detection method[c]	substrate present
1	k_1	22.0 ± 4.0	21 ± 10	DA	8.75 mM C_2H_2
2	k_2	27.5 ± 3.0	42 ± 10	DA	8.75 mM C_2H_2
3	k_2[b]	29.1 ± 1.0	45 ± 3	SW	none
4	k_2	25.6 ± 3.6	33 ± 13	DA	none
5	(k_2)[d]	28 ± 5	40 ± 12	SW	150 μM CH_4, <17 °C
6	(k_2)[d]	36.7 ± 3.0	68 ± 10	SW	75 μM C_2H_2, <16 °C
7	k_3[b]	14.2 ± 1.0	-15 ± 3	SW	none
8	k_3	8.7 ± 2.5	-30 ± 9	DA	none
9	(k_3)[d]	7.3 ± 1.0	-29 ± 5	SW	150 μM CH_4, >17 °C
10	k_3	10.7 ± 0.9	-24 ± 3	SW	300 μM CD_4
11	(k_3)[d]	11.6 ± 1.6	-16 ± 5	SW	75 μM C_2H_2, >16 °C
12[e]	k_3	20.5	19		300 μM CH_4
13[e]	k_3	24.0	26		300 μM CD_4

[a] k_1, k_2, and k_3 refer to H_{peroxo} formation, H_{peroxo} decay/Q formation, and Q decay, respectively. [b] These values agree reasonably well with the previously reported values determined under similar conditions (ref 11): $\Delta H^{\ddagger} = 27$ kcal/mol and $\Delta S^{\ddagger} = 35$ cal/mol·K for k_2 and $\Delta H^{\ddagger} = 18$ kcal/mol and $\Delta S^{\ddagger} = 2$ cal/mol·K for k_3. [c] DA: data obtained by using a Xe lamp with diode array detection. SW: data obtained by using monochromatic light with photomultiplier tube detection. [d] The kinetic steps corresponding to these activation parameters were not identified. The origin of the assignments is described in the Discussion section. [e] Values from *Ms. trichosporium* OB3b obtained by replotting the Arrhenius data from ref 62 in an Eyring format.

was detected after a single turnover, however, in a quantity corresponding to about 30% of the protein active sites in the presence of protein B and about 20% of those sites in its absence. This result reveals that, in the absence of substrate, at least some of the iron centers evolve hydrogen peroxide. The fate of the other oxidizing equivalents is unknown, and we have no evidence that MMO acts as a catalase.[12] It is also possible that the buffer is oxidized by Q, although no changes in Q decay rate were observed when using MES, MOPS, and Tris.[41]

The temperature dependence of rate constants for the formation and decay of Q in the absence of substrate was investigated. Rate constants were measured by using broadband radiation from a xenon lamp with diode array detection or monochromatic radiation from a quartz−halogen lamp and monochromator (λ = 420 nm) with a photomultiplier detector (Figure S1, Supporting Information). In both cases, the data at each wavelength fit well to rate constants for a single-exponential formation and a single-exponential decay. Activation parameters for formation and decay of Q obtained from the Eyring plots are provided in Table 1 as entries 3, 4, 7, and 8.

The decay of intermediate Q was much faster when the 75-W xenon lamp was employed to obtain diode array data as compared to the 30-W quartz−halogen lamp used for single-wavelength studies. Figure 3 displays kinetic traces reflecting this rate enhancement. This photoreaction is also evident in the different activation parameters for the decay of Q (Table 1, entries 7 and 8).

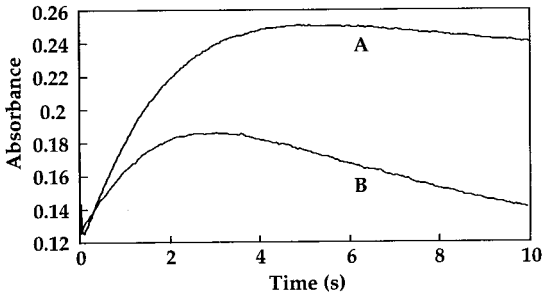

Figure 3. Formation and decay of Q at 4 °C when irradiated with (A) 420-nm light from a 30-W quartz−halogen lamp and (B) a 75-W xenon lamp. Rate constants of formation and decay are (A) $k_{form} = 0.43$ s^{-1} and $k_{decay} = 0.06$ s^{-1} and (B) $k_{form} = 0.43$ s^{-1} and $k_{decay} = 0.24$ s^{-1}.

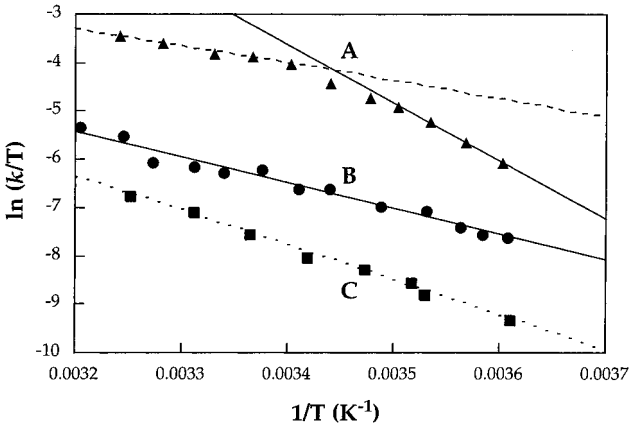

Figure 4. Eyring plots for decay of the absorbance at 420 nm after mixing H_{red}/2B with dioxygen and substrate at pH 7. (A) Nonlinear Eyring plot derived from optical decay rates at 420 nm upon mixing H_{red}/2B with a solution of dioxygen and 150 μM methane. (B) Eyring plot for Q decay in the presence of 300 μM CD_4. (C) Eyring plot for Q decay in the absence of substrate. The 30-W quartz−halogen lamp was used to obtain these data.

Kinetic Studies of Intermediate Formation and Decay in the Presence of Methane. As stated above, the decay rate of intermediate Q is accelerated in the presence of substrates. To obtain activation parameters for the reaction of Q with methane, kinetics were monitored at 420 nm in a manner identical to that used for similar studies in the absence of substrate.[11] The data for "Q decay," obtained in the presence of 150 μM methane from 4.4 to 35.3 °C, resulted in a nonlinear Eyring plot with an inflection point near 17 °C (Figure 4A). The activation parameters obtained from the two regions of the Eyring plot are substantially different (Table 1, entries 5 and 9). Based on previous single-turnover experiments, decay of the optical feature at 420 nm was presumed to arise solely from decay of intermediate Q. In fact, this correlation is not always the case (see Discussion).

The temperature dependence of Q decay was also monitored at 420 nm in the presence of 300 μM methane-d_4. In this case, a linear Eyring plot was obtained (Figure 4B), leading to activation parameters similar to those obtained above 17 °C for methane (Table 1, entry 10).

The dependence of the decay kinetics on methane concentration, monitored at 420 nm, was examined at 7.7 and 23.8 °C, the two distinct regions of the nonlinear Eyring plot. At 7.7 °C, increasing [CH_4] had no effect on the decay rate at 420 nm (Figure 5A), whereas at 23.8 °C, the decay rate exhibited nearly

(38) A shoulder resulting from the Soret band of a cytochrome impurity is visible at 420 nm in the starting spectrum. From the expected extinction coefficient of such a component, 115−230 mM^{-1} cm^{-1} (Lemberg, R.; Barrett, J. *Cytochromes*; Academic Press: New York, 1973), we estimate its concentration to be <1% of the hydroxylase concentration. In control experiments in the absence of MMOB, there is a slight shifting of the Soret band of this cytochrome to higher energy, characteristic of heme iron oxidation. The magnitude of the optical change is very small compared to that of Q formation and decay, and it was therefore not identified as a separate process by global analysis in experiments with MMOB present.

(39) Salifoglou, A.; Lippard, S. J. Unpublished data.

(40) Coufal, D. E.; Wolf, S.; Biemann, K.; Lippard, S. J. Unpublished data.

(41) Abbreviations: H_{red}, diferrous MMO hydroxylase; H_{red}/2B, diferrous MMOH with 2 equiv of MMOB; H_{peroxo}, the diferric peroxo intermediate of MMOH; H_{ox}, the diferric form of MMOH; MES, 2-[*N*-morpholino]-ethanesulfonic acid; MOPS, 3-[*N*-morpholino]propanesulfonic acid; Tris, 2-amino-2-(hydroxymethyl)-1,3-propanediol; RFQ, rapid freeze quench.

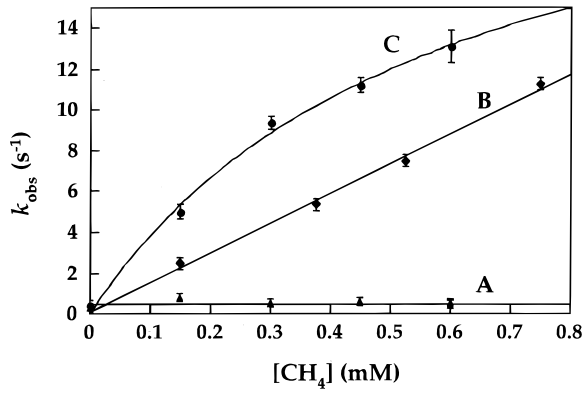

Figure 5. Methane concentration dependence of the kinetics of optical decay at 420 nm at 7.7 (A) and 23.8 °C (C) obtained upon reaction of H_{red}/2B with a solution of dioxygen and methane under single-mixing conditions. Plot B reveals the methane concentration dependence of Q decay monitored under double-mixing conditions at 7.8 °C. In this case, intermediate Q was generated in the initial push and, after a 1.5-s delay, was mixed with buffer containing methane. Curve fitting is described in the text. The 75-W xenon lamp was used in these experiments.

first-order dependence at low [CH_4] and began saturating at higher [CH_4] (Figure 5C).

The reaction between Q and methane could be investigated directly with double-mixing stopped-flow methodology. In these experiments, Q was formed by reaction of H_{red} with dioxygen in the absence of substrate; then, following an appropriate time delay, the solution of Q was rapidly mixed with methane. The appropriate delay times were determined by examining the dioxygen activation reaction in the absence of methane and identifying the time at which maximal Q concentration was achieved. Under these conditions, the optical decay rate at 420 nm exhibited a first-order dependence on methane concentration at 7.7 °C (Figure 5B). In addition, temperature dependence studies afforded a linear Eyring plot over the entire temperature range, 4.2−32.9 °C (Figure S2).

The reaction between Q and methane was also examined in a single-mixing experiment employing diode array rather than single wavelength detection. In the presence of 300 μM methane at 23.8 °C, the kinetic data required four independent species to achieve an acceptable fit (Figure 6A,B) based on an A → B → C → D kinetic model, that is H_{red} → H_{peroxo} → Q → H_{ox}. The diode array spectra of the individual species obtained by global analysis were nearly equivalent to those obtained for the single-turnover reaction in the absence of substrate (Figures 2A and S3). At 7.7 °C, however, the kinetic data fit an A → B → C model (Figure 6C), and the diode array spectra of the three species corresponded to H_{red}, H_{peroxo}, and H_{ox}, respectively (Figures 2A and S3). Intermediate Q did not build up to an appreciable extent under these conditions.

Kinetic Studies of Intermediate Formation and Decay in the Presence of Acetylene. The kinetics of Q decay in the presence of 75 μM acetylene were monitored at 420 nm at temperatures ranging from 3.2 to 35.3 °C. An Eyring plot (Figure S4) generated from the data again revealed nonlinear behavior with an inflection point at ∼16 °C. Activation parameters were determined in both temperature regimes (Table 1, entries 6 and 11).

At higher acetylene concentrations, it was possible to obtain a linear Eyring plot for kinetics only associated with H_{peroxo} formation and decay (Figure S5). In reactions containing 8.75 mM acetylene, Q did not accumulate, based on global analysis of diode array spectral data. Activation parameters determined

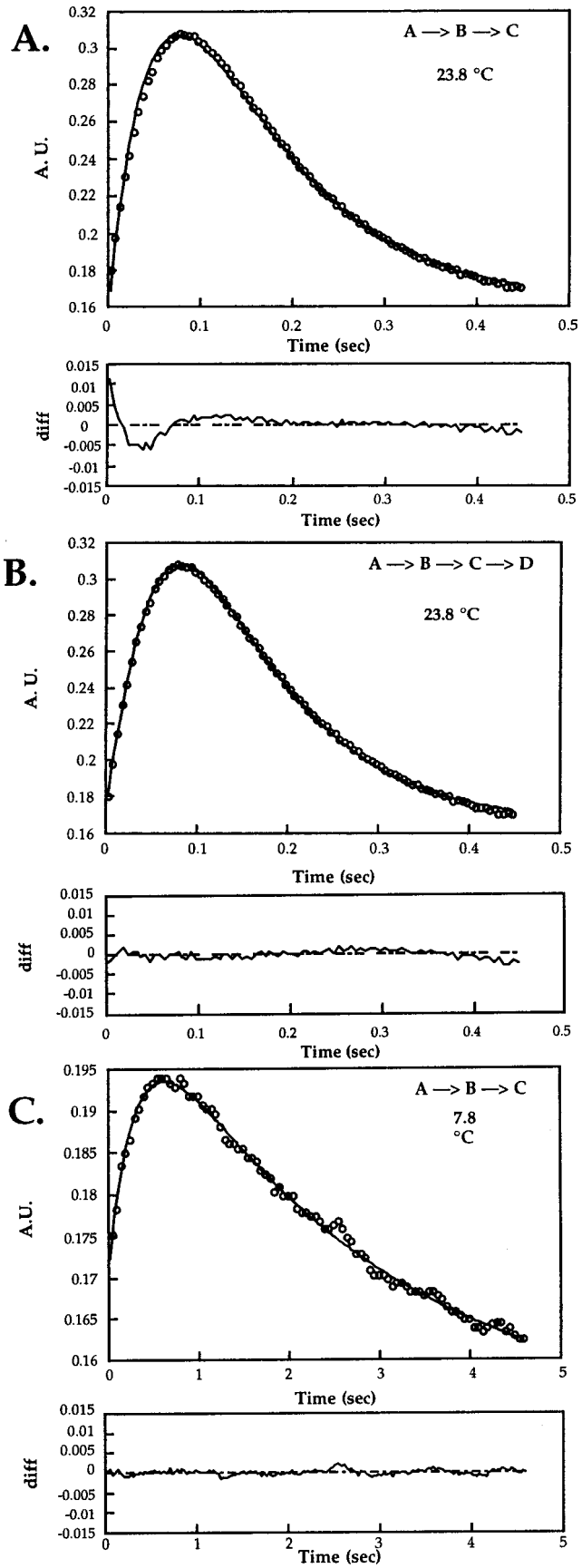

Figure 6. Evolution of absorbance at 420 nm after mixing H_{red}/2B with buffer containing dioxygen and 300 μM CH_4. (A and B) At 23.8 °C, the data fit best to a model involving four spectroscopically distinct species, that is, an A → B → C → D model. (C) At 7.8 °C, an A → B → C model is sufficient to fit the data. The identities of the various species are outlined in the text.

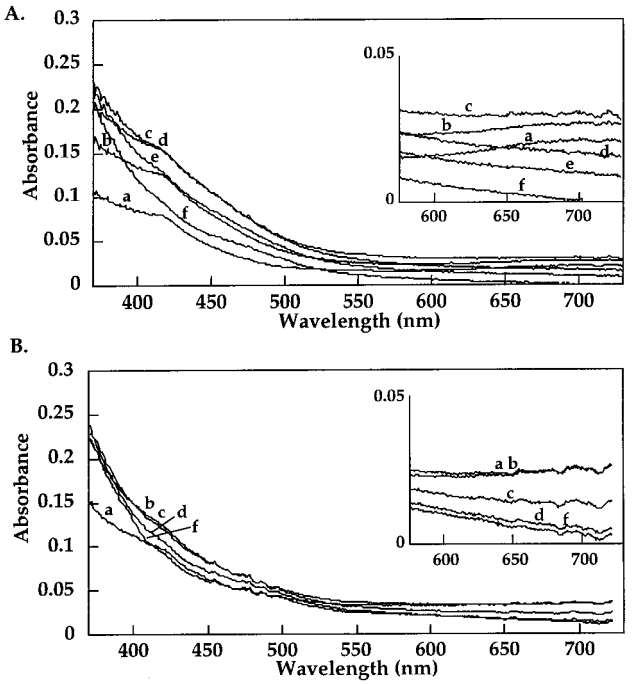

Figure 7. Diode array spectra after mixing H_{red}/2B with dioxygen and 1 mM methane (A) or 3 mM propylene (B) and dioxygen at 20 °C. Spectra correspond to (a) 15, (b) 45, (c) 75, (d) 135, (e) 195, and (f) 285 ms of reaction time.

for H_{peroxo} formation and decay in the presence of 8.75 mM acetylene are listed in Table 1, entries 1 and 2, respectively.

The dioxygen concentration dependence of H_{peroxo} formation and decay rates was examined at 4 °C with 8.75 mM acetylene present (Figure S6). Within experimental error, no dioxygen dependence was observed for either rate, suggesting that at least one kinetic step involving dioxygen precedes the formation of H_{peroxo}.

Reactions of Intermediate Species with Substrates. Stopped-Flow Optical Spectroscopy. As indicated above, much less intermediate Q accumulated when single-mixing stopped-flow experiments were performed with methane or acetylene present than when no substrate was present. This observation is displayed graphically in Figure 7A (cf. Figure 1 and the buildup at 420 nm). Furthermore, the rate of Q decay depended on the identity and concentration of substrate, in agreement with earlier reports.[11,16] When olefins were used as substrates, the same effect was observed, but the apparent extinction coefficient of Q as determined by global analysis decreased with increasing olefin concentration. This result suggests less Q formation. At the highest concentrations of olefin, the rate of decay of H_{peroxo} also increased (Figure 7B). In single-turnover experiments with substrate, the final oxidized spectrum displayed a shoulder at 480 nm. Addition of propylene oxide to H_{ox} in the presence of MMOB did not produce this shoulder.

Double-mixing stopped-flow experiments were performed to allow buildup of intermediate species, followed by rapid mixing with substrate. In this manner, we were able to monitor independently the interaction between H_{peroxo} and Q with substrate. The double-mixing technique has the added advantage that reaction of reduced protein with dioxygen takes place in an aging loop, where the protein is not irradiated to accelerate the rate of Q decay. Under such conditions, more Q accumulated than in a typical single-mixing experiment, even a single-mixing experiment in the absence of substrate. Experiments were carried out at 20 °C with varying delay times. Typically, for reactions

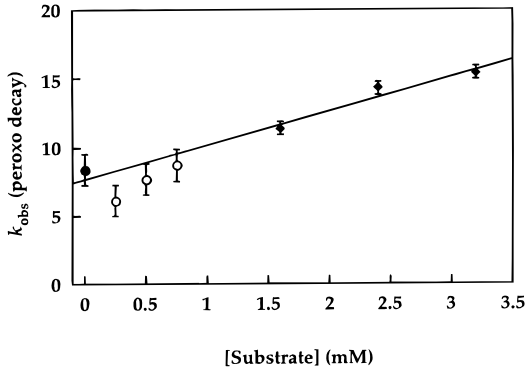

Figure 8. Plot of k_{obs} for H_{peroxo} decay vs [propylene] (◆) and [methane] (○) obtained by diode array spectroscopy. Error bars represent ±1 standard deviation. The concentration range for methane was limited by its solubility in water.

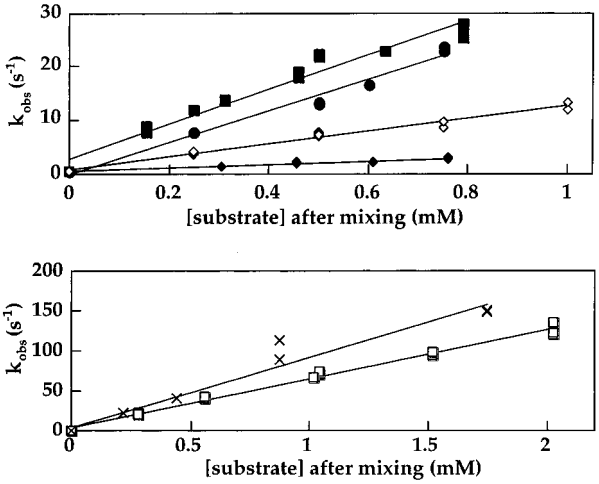

Figure 9. Plot of k_{obs} for the decay of Q vs [substrate] at pH 7 and 20 °C monitored by diode array spectroscopy. Substrates tested were methane (●), ethane (■), propane (◆), ethylene (□), propylene (◇), and acetylene (×).

with H_{peroxo}, the delay time was 35−40 ms at 20 °C, and for reactions with Q, the delay time was 400 ms (see Figure 2B).

In such a double-mixing experiment, propylene caused the H_{peroxo} signal to disappear in a concentration-dependent manner (Figure 8). For methane, the results are less obvious. Within the available methane concentration range, the H_{peroxo} decay rate does not exceed that observed in the absence of substrate. The change in H_{peroxo} decay rates with propylene concentration is clear within the uncertainty of the experiment (Figure 8). Unfortunately, the limited solubility of methane in water restricted the concentration range accessible to these experiments. GC analysis of the solution after such a single-turnover experiment with propylene revealed only propylene oxide formation, irrespective of the delay time before propylene addition. No allyl alcohol was detected. The Q optical signal decayed with a first-order dependence on substrate concentration for all substrates tested (Figure 9). Second-order rate constants for the reaction between Q and the various substrates are presented in Table 2. Representative primary data used to obtain the values in Table 2 are presented in Figure S7.

Discussion

Spectroscopic Characterization of H_{peroxo}. Figure 2A depicts the optical spectrum of the H_{peroxo} intermediate. Like many peroxo-bridged diiron(III) model compounds[17−19,42−45] and the recently identified peroxo intermediates in a ribonucle-

Table 2. Reaction Order in Substrate and Second-Order Rate Constants for the Reactions of Substrates with Intermediate Q at 20 °C

substrate	reaction order in substrate	k ($\times 10^4$ M^{-1} s^{-1})
methane	1.10	2.9
ethane	0.73	3.2
propane	0.70	0.31
ethylene	0.90	6.1
propylene	0.83	1.2
acetylene	0.90	8.8

otide reductase mutant,[46] frog M ferritin,[47] and stearoyl-ACP Δ^9-desaturase,[48] H_{peroxo} exhibits a very broad absorbance (λ_{max} = 725 nm, $\epsilon \approx 1800$ M^{-1} cm^{-1}) characteristic of a peroxo-to-iron(III) charge-transfer transition.[49] Its extinction coefficient was calculated on the basis of the total MMOH concentration and not corrected for protein inhomogeneity. From RFQ Mössbauer experiments,[50] which interrogate concentration changes in diiron species during the reaction of H_{red}/2B with dioxygen, we estimate that, at most, 70% of the protein forms the H_{peroxo} intermediate. Because there is no simple way to know the productive population for each stopped-flow experiment, however, the data are not corrected. The extinction coefficient also does not take into account the fact that there are two active sites per protein molecule. As for the diiron(III) peroxo species in Δ^9-desaturase,[48] a broad absorption feature was also observed at higher energy, ~400 nm (Figure 2A,C). A spectroscopic and theoretical study of the related diiron(III) peroxo model compound, $[Fe_2(\mu\text{-}O_2)(\mu\text{-}O_2CPh)_2\{HBpz'_3\}_2]$, assigned absorption bands in this region to peroxide-to-iron charge-transfer transitions.[49] The H_{peroxo} intermediate is most likely a (μ-1,2 peroxo)diiron(III) species. Its Mössbauer parameters (δ = 0.66 mm/s, ΔE_Q = 1.51 mm/s)[11,13] most resemble those of peroxo intermediates generated for a D84E RNR mutant and frog M ferritin[46,47] as well as a structurally characterized model compound.[17] In the model, $[Fe_2(\mu\text{-}O_2)(\mu\text{-}O_2CCH_2Ph)_2\{HBpz'_3\}_2]$, where pz′ = 3,5-bis(isopropyl)pyrazolyl, the peroxide moiety bridges the two iron atoms in a gauche μ-1,2 fashion, with an Fe−O−O−Fe dihedral angle of 52.9°. Theoretical studies of H_{peroxo}[22,24,51,52] together with recent resonance Raman data on the peroxo species in the RNR mutant[53] and stearoyl-ACP Δ^9-desaturase[48] also support a μ-1,2 binding mode. Therefore, this structural model remains the preferred one for H_{peroxo} (Scheme 1).

Q Formation and Decay in the Absence of Substrates. Activation parameters for Q formation and decay have been previously reported,[11] but the experiments were repeated for several reasons. A larger proportion of active hydroxylase is available from recent enzyme preparations, as determined by Mössbauer quantitation. In addition, we wished to check whether greater quantities of cytochrome impurities (up to 5 mol %) in earlier enzyme preparations may have interfered with single-wavelength kinetics at 420 nm.[38] The activation parameters determined here (Table 1, entries 3 and 7) are similar to those reported previously, although the present entropy of activation for Q decay has a negative sign, −15 eu, compared to the 2 eu value determined previously. The revised value is more consistent with that obtained when substrates are present (see below).

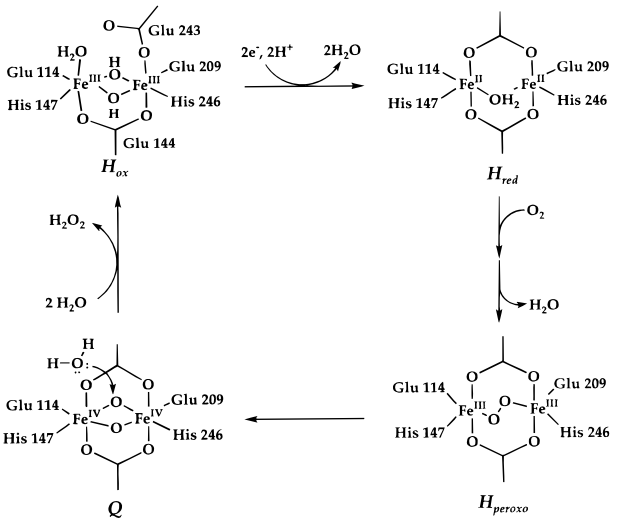

Figure 10. Proposal for the species observed in the single-turnover reaction of H_{red}/2B with O_2 in the absence of substrate.

Figure 10 depicts our proposal for the species observed in a single-turnover reaction in the absence of a hydrocarbon substrate. The resting enzyme, shown in the di(μ-hydroxo)-diiron(III) form (H_{ox}),[21] is converted to the diiron(II) state H_{red} by addition of two electrons from dithionite and two protons. The structure shown for the reduced hydroxylase is that recently observed by X-ray crystallography.[54] Initial reaction of the diiron(II) hydroxylase with dioxygen is rapid and not observed by any of the methods employed thus far. The fact that H_{peroxo} formation is independent of dioxygen concentration implies the presence of an unobserved initial step, such as formation of a tightly bound H_{red}/O_2 Michaelis complex. Studies of the *Ms. trichosporium* OB3b system also support the existence of such a step.[55] Formation of H_{peroxo} might occur with concomitant release of water, which would account for the positive entropy of activation determined for this step (see below).

H_{peroxo} next converts to Q, which is represented as a bis(μ-oxo)bis(μ-carboxylato)diiron(IV) unit. This quadruply bridged structure is proposed on the basis of recent synthetic model studies in which a di(μ-carboxylato)diiron(II) model compound reacts with dioxygen to form a di(μ-hydroxo)bis(μ-carboxylato)-diiron(III) product having just such a tetra-bridged geometry and a short Fe···Fe distance of 2.86 Å.[56] Additional oxidation to a diiron(IV) state would further shorten the distance, possibly to the value of 2.45 Å reported from EXAFS experiments.[20] In sMMO, conversion to Q might require side-chain movements to accommodate such a geometry, which might account for the

(42) Kitajima, N.; Tamura, N.; Amagai, H.; Fukui, H.; Moro-oka, Y.; Mizutani, Y.; Kitagawa, T.; Mathur, R.; Heerwegh, K.; Reed, C. A.; Randall, C. R.; Que, L., Jr.; Tatsumi, K. *J. Am. Chem. Soc.* **1994**, *116*, 9071−9085.
(43) Feig, A. L.; Lippard, S. J. *Chem. Rev.* **1994**, *94*, 759−805.
(44) Feig, A. L.; Becker, M.; Schindler, S.; van Eldik, R.; Lippard, S. J. *Inorg. Chem.* **1996**, *35*, 2590−2601.
(45) LeCloux, D. D.; Barrios, A. M.; Mizoguchi, T. J.; Lippard, S. J. *J. Am. Chem. Soc.* **1998**, *120*, 9001−9014.
(46) Bollinger, J. M., Jr.; Krebs, C.; Vicol, A.; Chen, S.; Ley, B. A.; Edmondson, D. E.; Huynh, B. H. *J. Am. Chem. Soc.* **1998**, *120*, 1094−1095.
(47) Pereira, A. S.; Small, W.; Krebs, C.; Tavares, P.; Edmondson, D. E.; Theil, E. C.; Huynh, B. H. *Biochemistry* **1998**, *37*, 9871−9876.
(48) Broadwater, J. A.; Ai, J.; Loehr, T. M.; Sanders-Loehr, J.; Fox, B. G. *Biochemistry* **1998**, *37*, 14664−14671.
(49) Brunold, T. C.; Tamura, N.; Kitajima, N.; Moro-oka, Y.; Solomon, E. I. *J. Am. Chem. Soc.* **1998**, *120*, 5674−5690.
(50) Valentine, A. M.; Pereira, A.; Tavares, P.; Huynh, B. H.; Lippard, S. J. Unpublished results.
(51) Yoshizawa, K.; Hoffmann, R. *Inorg. Chem.* **1996**, *35*, 2409−2410.
(52) Yoshizawa, K.; Yokomichi, Y.; Shiota, Y.; Ohta, T.; Yamabe, T. *Chem. Lett.* **1997**, 587−588.
(53) Moënne-Loccoz, P.; Baldwin, J.; Ley, B. A.; Loehr, T. M.; Bollinger, J. M., Jr. *Biochemistry* **1998**, *37*, 14659−14663.
(54) Whittington, D. A.; Lippard, S. J. Unpublished results.
(55) Liu, Y.; Nesheim, J. C.; Lee, S.-K.; Lipscomb, J. D. *J. Biol. Chem.* **1995**, *270*, 24662−24665.
(56) Lee, D.; Lippard, S. J. *J. Am. Chem. Soc.* **1998**, *120*, 12153−12154.

positive entropy of activation. The sizable enthalpy of activation is consistent with cleavage of the O−O bond to generate a high-valent diiron intermediate. The interpretation of the activation parameters in these reactions must be viewed with caution, however. Protein complexes between MMOH and MMOB are required for the catalytic reaction**,** and changes in the nature of this interaction and/or protein complex dissociation in any of the reaction steps would most likely influence the activation parameters. Furthermore, the energetics of such protein−protein interactions may exhibit temperature-dependent changes.

In the absence of substrate, small amounts of hydrogen peroxide (20−30%) are generated in single-turnover reactions. The mechanism of hydrogen peroxide formation may involve either protonation of a diferric peroxo species or nucleophilic attack by water on the electrophilic, high-valent intermediate Q.[47] The latter possibility is depicted in Figure 10. The lower activation energy for the light-promoted Q decay reaction might reflect generation of a ligand-to-metal charge-transfer excited state that is more susceptible to nucleophilic attack by water. With or without photoactivation, the bimolecular reaction proceeds with negative entropy and only modest enthalpy of activation. Release of hydrogen peroxide regenerates the diiron(III) form of the enzyme. Precedent for this conversion is provided by the structurally similar ferroxidase center of ferritin, in which hydrogen peroxide forms in the reaction of the diferrous protein with dioxygen.[57−59]

The physiological relevance of the hydrogen peroxide formation is uncertain. In cytochrome P450, the catalytic reaction is not fully coupled; some fraction of the turnovers results in hydrogen peroxide formation rather than substrate oxygenation.[60] In sMMO, hydrogen peroxide is not produced under steady-state turnover conditions, except at high MMOR/MMOH ratios. In the absence of hydrocarbon substrates, sMMO oxidase activity produces water rather than hydrogen peroxide.[12] When substrates are present, this oxidase activity competes with substrate oxidation, and fully coupled catalytic turnover arises only at kinetically saturating substrate concentrations.[12,61] The most prominent difference between the single-turnover and steady-state sMMO reactions without substrate is the availability of electrons from NADH/MMOR in the latter case. Reduction of Q or H_{peroxo} by electron transfer from MMOR or reduction of hydrogen peroxide generated in the active site produces water and the diiron(III) resting state, H_{ox}. Such reactions enable the cell to avoid accumulation of hydrogen peroxide in the cytoplasm.

Kinetic Studies of the Formation and Decay of Q in the Presence of Methane. Although methane is the physiologically relevant substrate for sMMO, much of the mechanistic information about this enzyme has come from studies of other hydrocarbons. In the present work, we have investigated the methane oxidation step in further detail. From the temperature dependence of Q decay in the presence of methane, a nonlinear Eyring plot was unexpectedly obtained (Figure 4A). Above 17 °C, the activation parameters resembled values measured in the absence of substrate (cf. Table 1, entries 7 and 9). Very different values were obtained below 17 °C, however, and are similar to those reported for methane oxidation by Q in sMMO from *Ms. trichosporium* (OB3b), for which a linear Arrhenius plot was obtained over the narrow temperature range of 1.8−7.0 °C (cf. Table 1, entries 5 and 12).[62]

Scheme 2

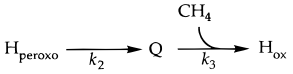

Several possible explanations for the nonlinear behavior were considered,[63] two of which seemed most plausible. One is that the MMOH/2MMOB complex may exist in two distinct conformations that exhibit different activities. If there were a large temperature-dependent equilibrium constant relating these states, the relatively sharp break in the Eyring plot might arise.[64] Alternatively, the kinetics, as monitored at 420 nm, might reflect two successive reactions with different activation parameters. In such a case, the rate-limiting step might change with temperature.

To distinguish between these possibilities, we examined the temperature dependence of the reaction of Q with CD_4. We reasoned that use of deuterated methane would significantly perturb only the C−H activation step and thus may facilitate interpretation of the Eyring plot. The Eyring plot generated from these experiments was linear from 4 to 39 °C (Figure 4B). Since substrate deuteration should have no effect on protein conformation, this result argues against the existence of two conformers with different reactivity being the basis of the nonlinear Eyring plot. In addition, the activation parameters obtained for CD_4 oxidation are very similar to those for methane above 17 °C, exhibiting only slightly higher activation enthalpy (Table 1, entries 9 and 10). Further insights were provided by studies of the dependence of the reaction on methane concentration at high, 23.8 °C, and low, 7.7 °C, temperatures. Figure 5A,C reveals that the reaction depends on $[CH_4]$ at 23.8 °C but not at 7.7 °C, results that support a two-step sequence for methane activation. The first step is rate limiting at low temperature, and the second, $[CH_4]$-dependent step is rate limiting at higher temperature. This mechanism is depicted in Scheme 2, and the data in Figure 5C are fit to the kinetic rate expression (eq 2) for such a sequence. The derived rate constants are $k_2 = 26 \pm 3\ s^{-1}$ and $k_3 = (4.5 \pm 0.4) \times 10^4\ M^{-1}\ s^{-1}$ at 23.8 °C.

$$\nu = \frac{k_2 k_3 [\mathrm{MMOH}]_0 [\mathrm{CH_4}]}{k_2 + k_3 [\mathrm{CH_4}]} \qquad (2)$$

To evaluate this hypothesis further, we investigated the reaction between Q and methane in the low-temperature range by double-mixing stopped-flow methods. In these experiments, the Q concentration was allowed to maximize prior to introduction of methane. Under these conditions, the rate of Q decay exhibited a first-order dependence on methane concentration at 7.7 °C (Figure 5B). Moreover, a linear Eyring plot was obtained over the entire 4.2−32.9 °C range (Figure S2), leading to activation parameters within experimental error of those derived from single-mixing experiments above 17 °C (Table 1, entry 9). These results are consistent with the proposed reaction sequence in Scheme 2. In the single-mixing experiments with methane below 17 °C, intermediate Q does not build up because the rate-limiting step is controlled by k_2. In contrast, k_3 controls the rate-limiting step at higher temperatures. Global fitting

(57) Xu, B.; Chasteen, N. D. *J. Biol. Chem.* **1991**, *266*, 19965−19970.
(58) Sun, S.; Arosio, P.; Levi, S.; Chasteen, N. D. *Biochemistry* **1993**, *32*, 9362−9369.
(59) Waldo, G. S.; Theil, E. C. *Biochemistry* **1993**, *32*, 13262−13269.
(60) Mueller, E. J.; Loida, P. J.; Sligar, S. G. In *Cytochrome P450: Structure, Mechanism, and Biochemistry*, 2nd ed.; Ortiz de Montellano, P. R., Ed.; Plenum: New York, 1995; pp 83−124.
(61) Stahl, S. S.; Lippard, S. J. Unpublished results.
(62) Nesheim, J. C.; Lipscomb, J. D. *Biochemistry* **1996**, *35*, 10240−10247.
(63) Dixon, M.; Webb, E. C. *Enzymes*, 3rd ed.; Academic Press: New York, 1979; pp 169−181.
(64) Massey, V.; Curti, B.; Ganther, H. *J. Biol. Chem.* **1966**, *241*, 2347−2357.

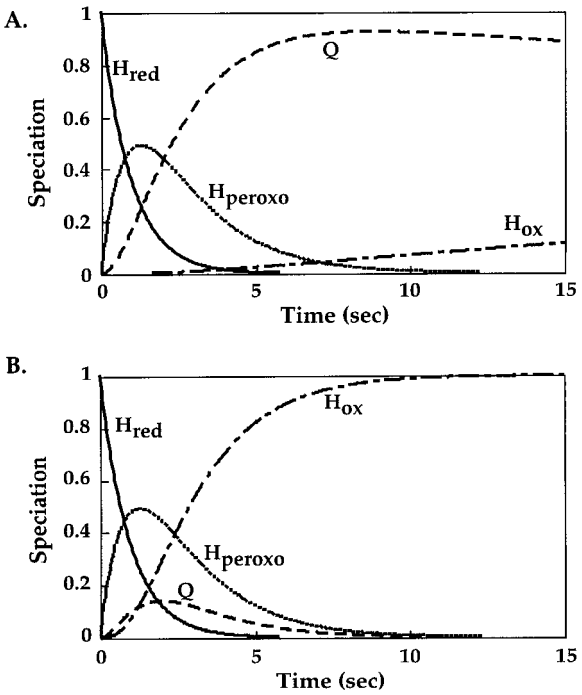

Figure 11. Time-dependent evolution of intermediates in a single-turnover reaction between H_{red}/2B and dioxygen in the absence (A) and in the presence (B) of 150 μM methane at 4 °C. The kinetic model, $H_{red} \rightarrow H_{peroxo} \rightarrow Q \pm CH_4 \rightarrow H_{ox}$, employed the following rate constants: $k_1 = 1.1\ s^{-1}$, $k_2 = 0.55\ s^{-1}$, k_3 ($-CH_4$) = $0.01\ s^{-1}$, and k_3 ($+CH_4$) = $1.7\ s^{-1}$. The enhanced Q decay rate in the presence of substrate is evidenced by the dramatically reduced accumulation of this intermediate in the reaction.

of the diode array data confirmed this analysis (Figures 6 and S3). When Q is generated independently and then mixed with methane at these temperatures, k_3 is the only reaction observed.

The Q decay rate in the presence of 150 μM methane at 4 °C was calculated by the Eyring equation and the activation parameters determined for the reaction above 17 °C. From this rate and the H_{peroxo} formation and decay rates measured at 4 °C, we constructed a plot of the time-dependent evolution of diiron species during the reaction (Figure 11B). A similar plot was generated for the single-turnover reaction at 4 °C in the absence of substrate (Figure 11A). The obvious difference between these plots is the quantity of Q that accumulates. In the presence of methane, Q is rapidly depleted and, at sufficient methane concentrations, virtually no Q builds up. The saturation behavior observed in Figure 5C indicates that the methane-independent conversion of H_{peroxo} to Q becomes partially rate limiting at high methane concentration, even at 23.8 °C.

More slowly reacting substrates such as CD_4 mask the unusual temperature-dependent behavior by permitting greater buildup of Q. In these cases, the decrease in optical density at 420 nm primarily corresponds to decay of Q rather than H_{peroxo}. From the rate constants obtained for reactions with CH_4 and CD_4, a kinetic isotope effect (KIE) for Q decay of ~28 at 4 °C was obtained.[65] Although this value is less than the KIE of 50−100 reported for the *Ms. trichosporium* (OB3b) system,[62] it is still larger than expected for a primary isotope effect that depends solely on differences between substrate zero-point energies.[66] Secondary isotope effects may also contribute, and ongoing studies seek to explore further the origin of this effect. The ability of substrate deuteration to alter the rate-determining step of an enzymatic reaction has been noted for lipoxygenase, which similarly exhibits a large primary isotope effect.[67]

(65) The CH_4 rate at 4 °C was obtained from the double-mixing stopped-flow experiments, 4.9 s^{-1}, and the CD_4 rate was obtained from single-mixing experiments, 0.14 s^{-1}. These values were normalized for the substrate concentrations, 0.38 mM CH_4 and 0.30 mM CD_4, and their ratio is the kinetic isotope effect.

Scheme 3

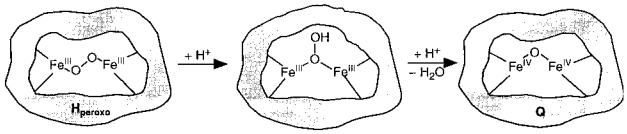

Scheme 4

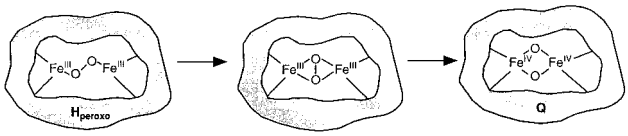

Conversion of H_{peroxo} into Q. One result arising from these studies is that, in the presence and in the absence of methane, the rate of H_{peroxo} formation is approximately 1−2 s^{-1} at 4 °C, a value considerably lower than 25 s^{-1} previously observed by RFQ Mössbauer spectroscopy[11,13] and stopped-flow optical methods.[14] Although the origin of this difference is not clear at present, one possibility is that two distinct forms of H_{peroxo}, which differ in their protonation states and/or coordination modes, are generated sequentially. This prospect suggests two ways by which H_{peroxo} may convert into intermediate Q (Schemes 3 and 4).

The first pathway, Scheme 3, resembles the mechanism proposed for cytochromes P450 and peroxidases, in which double protonation of a single oxygen atom releases water and generates a high-valent iron oxo species.[68] In sMMO, this high-valent intermediate contains two nearly equivalent Fe(IV) centers,[11,15] in contrast to the single Fe(IV) site and porphyrin radical cation that forms in heme-containing enzymes. Such a mechanism has been proposed recently for the conversion of a peroxo-bridged diiron(III) model complex into a more reactive oxidant.[49] Amino acid residues in the second coordination sphere, defined by the active site cavity, might play an important role in the conversion. Although this cavity comprises predominantly hydrophobic residues, the hydroxyl group of Thr213 lies within hydrogen-bonding distance of the water-derived ligands on iron.[7] By analogy to the role of a similarly positioned active-site threonine residue in cytochrome P450, Thr213 might serve as a proton shuttle for dioxygen activation. Active-site threonine residues are conserved among several other dioxygen-activating dinuclear iron enzymes, including toluene monooxygenase and stearoyl-ACP desaturases.[69]

The other pathway, depicted in Scheme 4, is analogous to the mechanism of dioxygen activation proposed for dicopper enzymes.[70−72] In this case, a μ-1,2 peroxo rearranges to a side-on-bound, μ-η^2:η^2 isomer, a conversion that may be facilitated by carboxylate shift(s) to open additional coordination sites on

(66) Melander, L.; Saunders: W. H., Jr. *Reaction Rates of Isotopic Molecules*; Krieger: Malabar, FL, 1987.
(67) Glickman, M. H.; Klinman, J. P. *Biochemistry* **1995**, *34*, 14077−14092.
(68) Sono, M.; Roach, M. P.; Coulter, E. D.; Dawson, J. H. *Chem. Rev.* **1996**, *96*, 2841−2887.
(69) Fox, B. G.; Shanklin, J.; Ai, J.; Loehr, T. M.; Sanders-Loehr, J. *Biochemistry* **1994**, *33*, 12776−12786.
(70) Solomon, E. I.; Sundaram, U. M.; Machonkin, T. E. *Chem. Rev.* **1996**, *96*, 2563−2605.
(71) Karlin, K. D.; Kaderli, S.; Zuberbühler, A. D. *Acc. Chem. Res.* **1997**, *30*, 139−147.
(72) Tolman, W. B. *Acc. Chem. Res.* **1997**, *30*, 227−237.

iron. Subsequent homolytic cleavage of the O−O bond would yield the corresponding bis(μ-oxo)diiron(IV) structure. As with cytochrome P450, the mechanism in Scheme 3 suggests that water elimination could provide the driving force needed to form the reactive oxidant Q. In contrast, Scheme 4 illustrates an explicit need for two metal centers to generate the reactive species which, if true, would support a unified mechanism for dioxygen activation by dinuclear iron and copper oxygenases. In this respect, it is interesting that a copper MMO exists,[73,74] but no metalloporphyrin-containing enzymes can oxidize methane. The structure depicted for the high-valent diiron species in Schemes 3 and 4 is consistent with the recent EXAFS data reported for intermediate Q and a recently reported model system.[20,56] Ongoing investigations seek to distinguish between these and other mechanistic possibilities.[21,43] Recent kinetic studies of the *Ms. trichosporium* sMMO system have led to similar considerations.[75]

Single-Turnover Kinetic Studies in the Presence of Acetylene. Because of its greater solubility than other small hydrocarbons in water, acetylene serves as a convenient substrate for single-turnover reactions. Acetylene is a suicide substrate for sMMO, covalently modifying the α subunits during steady-state turnover.[29] The protein retains 95% of its activity after a single-turnover reaction with acetylene,[76] however, and is therefore not inactivated during every cycle. Analysis of the temperature dependence of the optical decay rate at 420 nm at low acetylene concentration (75 μM) yielded a nonlinear Eyring plot, similar to that observed for methane. Prior to our obtaining this result, methane was the only substrate for which a nonlinear Eyring plot had been observed. It is now clear, however, that this behavior can arise with any substrate having sufficient solubility and reactivity to alter the rate-determining step in the single-turnover reaction.

At higher acetylene concentrations, formation and decay of H_{peroxo} is the only process observed by stopped-flow optical spectroscopy from 4 to 35 °C (Figure S5). The absence of Q greatly simplifies analysis of the optical kinetic data. We therefore determined the activation parameters for H_{peroxo} formation and decay in the presence of 8.75 mM acetylene by diode-array UV−visible spectroscopy (Table 1, entries 1 and 2). The H_{peroxo} formation rate at 4 °C is 6 ± 2 s^{-1}, a value higher than that observed in the presence of methane or no substrate (see above) but less than that obtained by RFQ Mössbauer spectroscopy**,** namely 25 s^{-1}.[11,13] It is possible that acetylene perturbs the active site or otherwise affects the H_{peroxo} formation kinetics.

It has already been reported that the rates of Q formation and decay do not depend on dioxygen concentration.[11] If H_{peroxo} were the immediate product of the reaction of H_{red} with dioxygen, its formation rate should depend on O_2 concentration. As indicated above, neither the formation nor the decay of H_{peroxo} ($\lambda_{max} = 725$ nm) depends on O_2 concentration when the reaction is carried out in the presence of 8.75 mM acetylene (Figure S6). This behavior differs from that obtained for structurally similar but sterically far less demanding diiron(II) model compounds, the O_2 reactions of which exhibit a first-order dependence on dioxygen concentration.[44,45] This result reinforces the hypothesis that there is at least one intermediate species formed before H_{peroxo} in the reaction cycle (Scheme 1) but does not address their identity or oxidation state. Such a species could be a Michaelis complex, similar to the postulated intermediate O,[55] a transient mixed-valent superoxo complex,[77] and/or the product of outer sphere electron transfer to dioxygen.[78−80]

Reactions of Substrates with Q. The data presented above and previous work by others[16,62] suggest that intermediate Q reacts directly with hydrocarbons to produce the oxidized substrate. The rate of Q decay accelerates in the presence of substrate and exhibits a first-order dependence on substrate concentration. Several hydrocarbons, including methane, ethane, propane, ethylene, propylene, and acetylene, were investigated here under double-mixing stopped-flow conditions. Each of the substrates reacts with Q, and their rate constants exhibit approximately linear concentration dependence (Figure 9). The second-order rate constants provided in Table 2 do not follow clear trends based on C−H bond strength or electron density, suggesting that substrate size must also play a role. This effect is illustrated by the rate of reaction of Q with ethane and propane at a given substrate concentration (Figure 9). If reaction of substrate with Q were to involve hydrogen atom abstraction, these two hydrocarbons, with the same primary C−H bond energy (98 kcal/mol), should react at similar rates. Propane might be expected to react even more rapidly because a weaker secondary C−H bond is available (95 kcal/mol). Steady-state oxidation of propane yields 39% of the primary alcohol and 61% of the secondary alcohol.[25] Nevertheless, propane reacts more slowly than ethane by an order of magnitude. Moreover, methane, which has a C−H bond strength of 104 kcal/mol, reacts more slowly than ethane but more rapidly than propane. Clearly, the reaction with alkanes depends on multiple factors. Similarly, Q reacts with propylene 5−6-fold more slowly than with ethylene. This difference is not electronic in origin, because propylene should be a better substrate for an electrophilic oxidant.

Acetylene reacts most rapidly with Q among all the substrates tested. The probable mechanism of acetylene activation is electrophilic oxidation to yield the oxirene[81,82] followed by product rearrangement[83,84] to a reactive ketene, which sometimes modifies the protein covalently and sometimes reacts with water to give acetic acid.[29] Figure 12 portrays possible mechanisms for oxidation of methane, propylene, and acetylene by Q, depicted as a bis(μ-oxo)diiron(IV) species.

Despite the apparent linearity of the plots in Figure 9, the corresponding log−log plots (Figure S8) reveal slight deviations of the slopes from unity, especially for the larger substrates (Table 2). This result can be explained by postulating a two-step mechanism[44] for the larger substrates. For example, if Q were in equilibrium with a more reactive form that required conformational change, the result could be a partial order with

(73) Nguyen, H.-H. T.; Nakagawa, K. H.; Hedman, B.; Elliott, S. J.; Lidstrom, M. E.; Hodgson, K. O.; Chan, S. I. *J. Am. Chem. Soc.* **1996**, *118*, 12766−12776.
(74) Nguyen, H.-H. T.; Elliott, S. J.; Yip, J. H.-K.; Chan, S. I. *J. Biol. Chem.* **1998**, *273*, 7957−7966.
(75) Lipscomb, J. D.; Lee, S.-K. Presented at the 216th National Meeting of the American Chemical Society, Boston, MA, August 1998; Paper INOR 197.
(76) Valentine, A. M.; Lippard, S. J. Unpublished results.
(77) Coufal, D. E.; Tavares, P.; Pereira, A. S.; Huynh, B. H.; Lippard, S. J. *Biochemistry* **1999**, *38*, in press.
(78) Dickerson, L. D.; Sauer-Masarwa, A.; Herron, N.; Fendrick, C. M.; Busch, D. H. *J. Am. Chem. Soc.* **1993**, *115*, 3623−3626.
(79) Francisco, W. A.; Tian, G.; Fitzpatrick, P. A.; Klinman, J. P. *J. Am. Chem. Soc.* **1998**, *120*, 4057−4062.
(80) Cohen, J. D.; Payne, S.; Hagen, K. S.; Sanders-Loehr, J. *J. Am. Chem. Soc.* **1997**, *119*, 2960−2961.
(81) Lewars, E. G. *Chem. Rev.* **1983**, *83*, 519−533.
(82) Ortiz de Montellano, P. R.; Kunze, K. L. *J. Am. Chem. Soc.* **1980**, *102*, 7373−7375.
(83) Scott, A. P.; Nobes, R. H.; Schaefer, H. F., III; Radom, L. *J. Am. Chem. Soc.* **1994**, *116*, 10159−10164.
(84) Termath, V.; Tozer, D. J.; Handy, N. C. *Chem. Phys. Lett.* **1994**, *228*, 239−245.

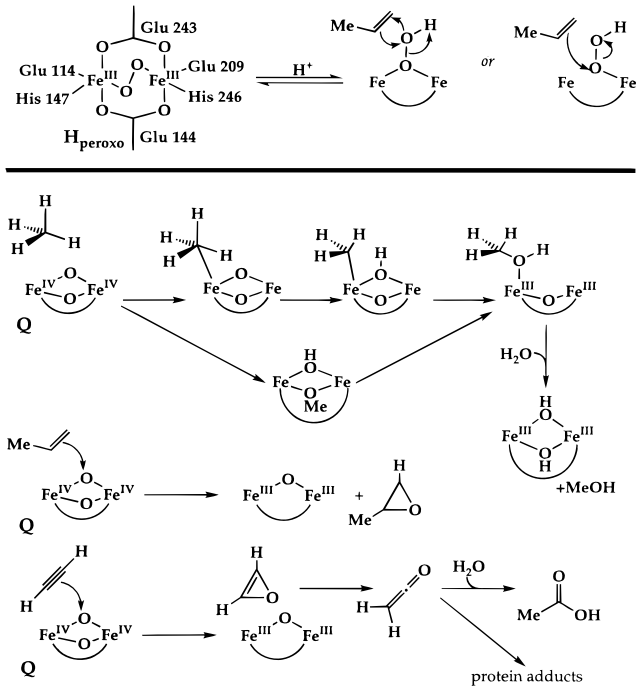

Figure 12. Possible mechanisms for (top) the reaction of propylene with H_{peroxo} and (bottom) the oxidation of methane, propylene, and acetylene by intermediate Q in sMMO.

respect to substrate. Alternatively, substrate binding to the enzyme followed by reaction with Q would lower the effective order.

Reactivity of Substrates with H_{peroxo}. Previous studies revealed that H_{peroxo} formation and decay are not affected by substrates.[11,16] The results presented here, however, suggest that H_{peroxo} can react directly with olefins, as manifested by the linear increase in the H_{peroxo} decay rate constant with increasing olefin concentration (Figure 8). This reactivity is also revealed by reduced accumulation of intermediate Q (Figure 7B). Accelerated conversion of H_{peroxo} to Q in the presence of olefin does not explain the data, because the rate constants for reactions of olefins with Q were measured directly in double-mixing experiments and are too modest (see above) to explain the decreased amount of Q that accumulates.

There is considerable precedent for olefin epoxidation by early transition metal peroxo species, usually requiring a high oxidation state for O atom transfer.[85,86] Low-valent, late transition metal peroxo species are typically nucleophilic,[87,88] and the H_{peroxo} intermediate has been predicted from model studies to be a nucleophile.[49] Protonation to form a hydroperoxide, however, would generate a more electrophilic oxidant (Scheme 3). A possible mechanism for the reaction of propylene with such a protonated form of H_{peroxo} is depicted in Figure 12.

Recent studies of cytochrome P450 have similarly reached the conclusion that multiple dioxygen activation intermediates can oxidize substrates.[89−91] The nature of the reactive oxidant depends on the substrate and/or the source of the enzyme. In cytochrome P450, epoxidation of cyclohexene and 2-butene was enhanced at the expense of allylic C−H hydroxylation in site-directed mutants, which disrupted the presumed proton-transfer pathway.[90] Based on this result, the authors suggested that a ferric hydroperoxo heme intermediate is capable of mediating epoxidation, whereas a high-valent compound I intermediate is necessary to effect C−H hydroxylation. The P450 mutant disfavors formation of the latter species. In sMMO, propylene hydroxylation is never observed; propylene oxide is the only product identified from the reaction mixture. Thus, even though hydroxylation of propylene could occur, it is not observed.

It is interesting to note that alkene monooxygenases (AMO) have been identified which are similar to sMMO in protein components, sequence homology, and putative diiron active sites.[92−94] These enzymes epoxidize propylene but do not hydroxylate alkanes. Furthermore, they are not inhibited by acetylene, which is a suicide substrate for sMMO[29] that reacts with Q but not with H_{peroxo} (see above). These results suggest that a Q-like intermediate may not form in the alkene monooxygenases, but instead, a peroxo diiron(III) species might oxidize the substrate. Such a mechanistic feature would account for the substrate specificity of these enzymes.

Conclusions

Stopped-flow experiments have provided new information about the intermediates in the catalytic cycle of sMMO and their reactions with substrates. The optical spectrum of H_{peroxo} and activation parameters for its formation are presented for the first time. The dioxygen independence of the formation rate constant supports the proposal that H_{peroxo} is not the initial product of the reaction of H_{red} with dioxygen. Further studies are necessary to identify the nature of such early intermediates.

Activation parameters for Q formation and decay were also investigated. When certain substrates are present in the single-turnover reactions, nonlinear Eyring behavior is observed for the kinetics monitored at 420 nm. In the past, optical absorption in this region has been exclusively ascribed to intermediate Q; however, H_{peroxo} also absorbs at this wavelength. Highly reactive substrates, such as methane and acetylene, are able to shift the rate-determining step of the single-turnover reaction such that kinetics at 420 nm reflect only H_{peroxo} reactions.

The reactions of substrates with Q in double-mixing stopped-flow experiments support the assignment of Q as an active oxidizing species. Several saturated and unsaturated hydrocarbons have been investigated. Contrary to assertions that substrates with stronger C−H bonds react more rapidly,[95] our results indicate that substrate reactivity trends are less predictable, arising from steric, electronic, and/or enzyme conformational factors that are presently poorly understood. Comparing the reactivity of saturated and unsaturated substrates seems less meaningful, based on their apparently distinct oxidation mechanisms. Finally, reactions with propylene indicate for the first

(85) Dussault, P. In *Active Oxygen in Chemistry*; Foote, C. S., Valentine, J. S., Greenberg, A., Liebman, J. F., Eds.; Chapman & Hall: New York, 1995; pp 141−203.
(86) Jacobsen, E. N. In *Comprehensive Organometallic Chemistry II, Vol 12*; Wilkinson, G., Stone, F. G. A., Abel, E. W., Hegedus, L. S., Eds.; Pergamon: New York, 1995; pp 1097−1135.
(87) Ho, R. Y. N.; Liebman, J. F.; Valentine, J. S. In *Active Oxygen in Biochemistry*; Valentine, J. S., Foote, C. S., Greenberg, A., Liebman, J. F., Eds.; Chapman & Hall: New York, 1995; pp 1−36.
(88) Selke, M.; Sisemore, M. F.; Ho, R. Y. N.; Wertz, D. L.; Valentine, J. S. *J. Mol. Catal. A* **1997**, *117*, 71−82.
(89) Vaz, A. D. N.; Pernecky, S. J.; Raner, G. M.; Coon, M. J. *Proc. Natl. Acad. Sci. U.S.A.* **1996**, *93*, 4644−4648.
(90) Vaz, A. D. N.; McGinnity, D. F.; Coon, M. J. *Proc. Natl. Acad. Sci. U.S.A.* **1998**, *95*, 3555−3560.
(91) Toy, P. H.; Newcomb, M.; Coon, M. J.; Vaz, A. D. N. *J. Am. Chem. Soc.* **1998**, *120*, 9718−9719.
(92) Small, F. J.; Ensign, S. A. *J. Biol. Chem.* **1997**, *272*, 24913−24920.
(93) Gallagher, S. C.; Cammack, R.; Dalton, H. *Eur. J. Biochem.* **1997**, *247*, 635−641.
(94) Gallagher, S. C.; George, A.; Dalton, H. *Eur. J. Biochem.* **1998**, *254*, 480−489.
(95) Lipscomb, J. D.; Que, L., Jr. *JBIC, J. Biol. Inorg. Chem.* **1998**, *3*, 331−336.

time that H_{peroxo} or related species may also oxidize substrates, converting propylene to propylene oxide. This observation may have implications for closely related enzymes, which are able to oxidize olefins but cannot oxidize alkanes.

Acknowledgment. This work was supported by a grant from the National Institutes of Health (GM32134), and S.S.S. acknowledges a postdoctoral fellowship from the National Science Foundation. We appreciated numerous helpful comments from Dr. G. T. Gassner as well as the reviewers.

Supporting Information Available: Figures S1−S8, displaying information described in the text (PDF). This material is available free of charge via the Internet at http://pubs.acs.org.

JA9839522